

Rotational Isomerism Involving an Acetylenic Carbon: Synthesis of and Barrier to Rotation around C(sp)–C(sp³) Bonds in Bis(1,4-disubstituted 9-triptycyl)ethynes

Shinji Toyota,* Takao Yamamori, Mitsuhiro Asakura, and Michinori Ōki

Department of Chemistry, Faculty of Science, Okayama University of Science, Okayama, 700-0005

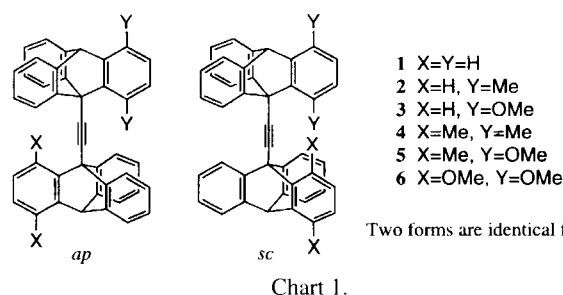
(Received August 5, 1999)

The substituent effect on the rotational barriers of acetylenic to tetrahedral C–C bonds was studied for the title compounds carrying Me or OMe substituents at the 1,4-positions in the 9-triptycyl groups. These compounds were prepared by use of the Diels–Alder and the Sonogashira reactions from a 9-ethynylantracene derivative. The kinetic parameters were determined by the total lineshape analysis of the signals observed by the variable temperature ¹H NMR for five compounds. The rotational barriers are in the range of 9–15 kcal mol^{–1}, and are enhanced as the steric size of the substituents is increased (H < OMe < Me). This substituent effect is attributed to the destabilization of the transition state of the rotation process, where the two triptycyl groups are almost eclipsed about the central axis, by the steric interactions between the *peri* substituents. The acetylenic carbons are significantly deformed from the linear geometry in the X-ray structure of the tetramethyl compound. The substituent effect on the rotamer population is also discussed with the aid of the MM calculation.

While the rotational isomerism about C–C single bonds formed between sp³ and sp² carbons has been extensively studied, little is known about that about C–C bonds involving at least one acetylenic sp carbon because of very low rotational barriers.^{1–4} For example, the insertion of an acetylenic moiety between two methyl groups considerably decreases the barrier height to rotation from ca. 3 kcal mol^{–1} for ethane⁵ to less than 10 cal mol^{–1} for 2-butyne⁶ (1 cal = 4.184 J). In the latter, the two terminal methyl groups are so far away (4.1 Å) that steric and stereoelectronic interactions are too little to furnish any meaningful rotational barrier.

Although the interaction can be increased by introducing bulky substituents at both ends of ethyne, the effective enhancement of the rotational barrier is very difficult due to the geometrical reasons. To the best of our knowledge, the only example of the restricted rotation at an acetylenic carbon in acyclic compounds was reported by Vögtle et al. for bis(9-triptycyl)ethyne derivatives.⁷ The rotational barrier of the tetramethyl compound (**4**) was determined by the NMR lineshape analysis as 15.6 kcal mol^{–1}; The unusually high barrier is attributed to the bulkiness of the 1-substituted triptycene groups. In order to discuss the substituent effect on the barrier height in detail, it is necessary to obtain additional kinetic data for the compounds with various substituents. Therefore, we determined the kinetic parameters for the C(sp)–C(sp³) bond rotation in the C–C≡C–C unit (hereafter designated as C–C bond for simplicity) in the title compounds with Me and OMe groups at the 1,4-positions, **2**–**6** (Chart 1), to contribute toward a systematic study of the rotational isomerism around bonds involving acetylenic sp carbons.

This paper reports a convenient route for the synthesis

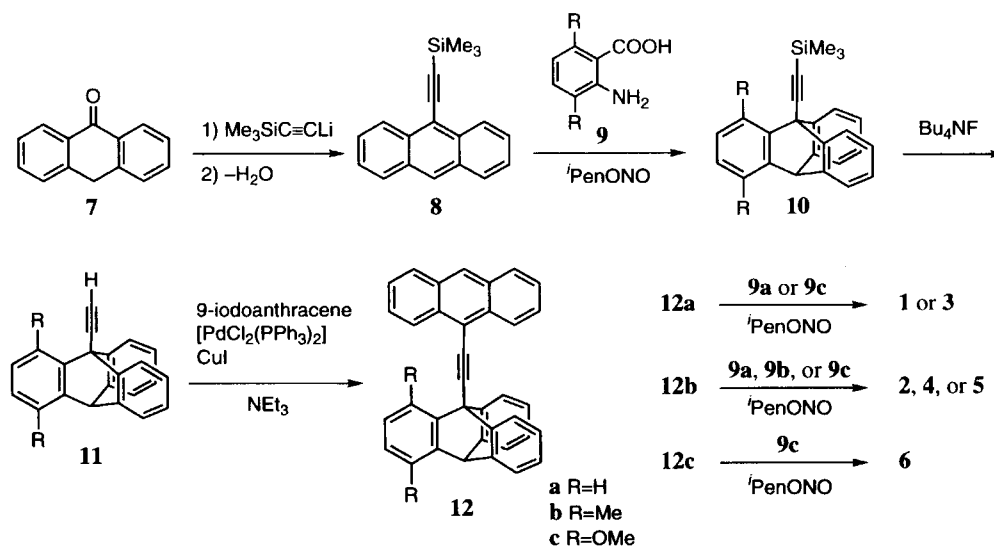


of the title compounds, especially those carrying different substituents on the two triptycyl groups (X ≠ Y). On the basis of the kinetic and thermodynamic data of the conformational change, and the molecular structures, the substituent effect on the rotational isomerism about the C–C bonds is discussed from various aspects.

Results

Synthesis. Compounds **1** and **4** had been synthesized by the Diels–Alder reaction of bis(9-anthryl)ethyne with a benzyne in the literature.⁷ This method was not always useful for the synthesis of unsymmetrically substituted compounds: **2**, **3**, and **5**. Therefore, we chose an alternative pathway involving the stepwise construction of each triptycene (Trip) skeleton by the Diels–Alder reaction and the connection of the acetylenic unit by the Sonogashira reaction (Scheme 1).⁸

9-[(Trimethylsilyl)ethynyl]anthracene (**8**) was prepared from 9-anthrone and lithium (trimethylsilyl)acetylide. The first triptycyl skeleton was constructed by the reaction of **8** with a substituted benzyne, generated from 3,6-disubstituted anthranilic acid (**9**) with isopentyl nitrite (*i*PenONO),



Scheme 1.

in reasonable yields. After the desilylation of **10** by fluoride, the terminal acetylene **11** was coupled with 9-iodoanthracene under conditions of the Sonogashira reaction. Thus formed 9-[(9-anthryl)ethynyl]triptycenes **12** were reacted with an appropriate benzyne to give the target compounds **1–6** in moderate yields with the recovery of a small to moderate amount of **12**. Compounds **2**, **3**, and **5**, in which $X \neq Y$, were prepared by the combination of **12** and **9** shown in Scheme 1, although the reaction of another combination was also available.

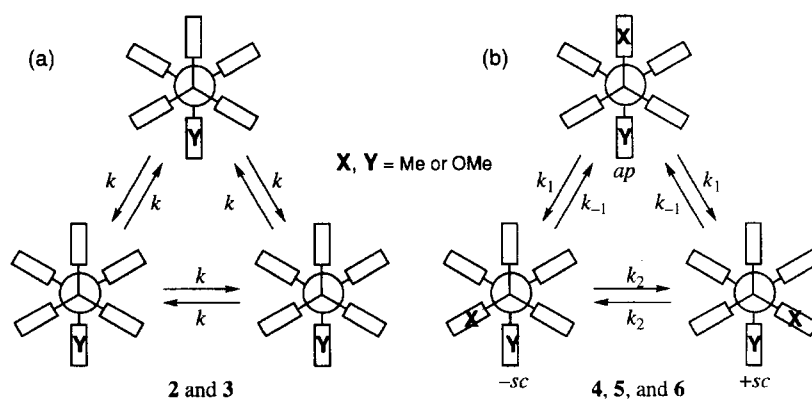
Kinetic and Thermodynamic Measurements by NMR.

The kinetic and thermodynamic parameters for rotation around the C–C bond were determined by the variable temperature NMR measurements except for **1**, which has no probe for the observation of the dynamic process. According to the substitution pattern, compounds **2–6** should exhibit two types of dynamic behavior, as illustrated in Scheme 2.

For **2** and **3**, in which $X = \text{H}$ and $Y \neq \text{H}$, there are three conformers of equal energy (Scheme 2(a)). Rotation around the C–C bond exchanges the magnetic sites of the three benzeno groups in the nonsubstituted Trip, in which one of them is *anti* to the substituent Y and the other two are *syn*, the mutual exchange among AAX systems taking place. This process

was observed as the lineshape changes of the signals due to the *peri* protons ($1'$, $8'$, and $13'$ -positions) in **2** (Fig. 1): A doublet at $\delta = 8.01$ observed at room temperature in CD_2Cl_2 broadened and separated into two doublets at $\delta = 7.73$ and 8.14 in 1 : 2 intensity as the temperature was lowered. The total lineshape analysis afforded the kinetic data of the bond rotation listed in Table 1. Although the methoxy compound (**3**) also showed a similar lineshape change at lower temperatures, the dynamic process was not completely frozen at the lowest attainable temperature, -110°C , in CD_2Cl_2 . The estimated free energy of activation was 8 kcal mol^{-1} for **3**.

The other type of dynamic behavior should be observed in **4–6**, where $X \neq \text{H}$ and $Y \neq \text{H}$. Among three conformers shown in Scheme 2(b), the *ap* form, in which X and Y are *anti*, has a different stability from the others, a pair of enantiomers of the *sc* form, in which X and Y are *gauche*.⁹ The analysis of the lineshapes due to the exchange between the unequally populated isomers gives the rates of bond rotation. For example, the tetramethyl compound (**4**) gave two kinds of signals in the ratio of 3.3 : 1 in CDCl_3 at -55°C , where the rate of rotation was sufficiently small. The isomers were unambiguously assigned by the signal pattern of the aromatic signals: The major and minor forms gave one and two sets



Scheme 2.

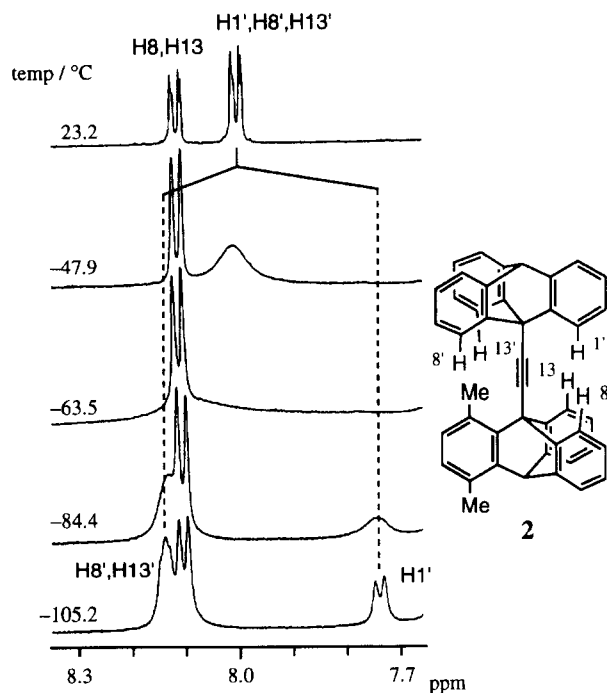


Fig. 1. ^1H NMR signals due to aromatic protons at the *peri*-positions in **2** at various temperatures (Solvent CD_2Cl_2).

Table 1. Kinetic Parameters for Rotation around C–C bonds in **2**–**6** in CD_2Cl_2 ^{a)}

Compound	ΔH^\ddagger	ΔS^\ddagger	ΔG_{273}^\ddagger
	kcal mol^{-1}	$\text{kcal mol}^{-1} \cdot \text{K}^{-1}$	kcal mol^{-1}
2	8.6 ± 0.3	-5.4 ± 1.2	10.1
3			8 ^{b)}
4 ^{c,d)}	15.1 ± 0.4	-1.1 ± 1.2	15.4
5 ^{c)}	11.2 ± 0.2	-5.1 ± 0.6	12.7
6 ^{c)}	9.4 ± 0.4	0.3 ± 1.9	9.3

a) 1 cal = 4.184 J. b) At 163 K. c) Data from *ap* to *sc* isomer.

d) In CDCl_3 .

of the signals due to the benzeno groups which do not carry any *peri* substituents, expected for the *ap* and *sc* isomers, respectively. This assignment is consistent with the low-field shift of the 1-Me signal ($\delta = 3.15$) in the *sc* isomer relative to that in the *ap* ($\delta = 2.65$) because the steric compression is

severe in the former. The rotamer ratio was monitored by the integral intensity of the signals due to each isomer at several temperatures where the exchange was slow, the data giving the thermodynamic parameters shown in Table 2. The lineshape changes were observed at higher temperatures (Fig. 2), and the lineshape analyses of the 1-Me proton signals afford the kinetic data listed in Table 1.

The thermodynamic and kinetic data for **5** and **6** were determined similarly (Tables 1 and 2). We could not obtain the details of the thermodynamic data of **6**, because the exchange between the isomers was not sufficiently slow, even at -105°C .

Molecular Structure. Among compounds **1**–**6**, only **4** gave crystals suitable for X-ray analysis by recrystallization from chloroform. An ORTEP drawing is shown in Fig. 3, in which solvent molecules are omitted. The selected structural parameters are listed in Table 3.

In order to get further structural information, the molecular mechanics (MM) calculations were carried out with the

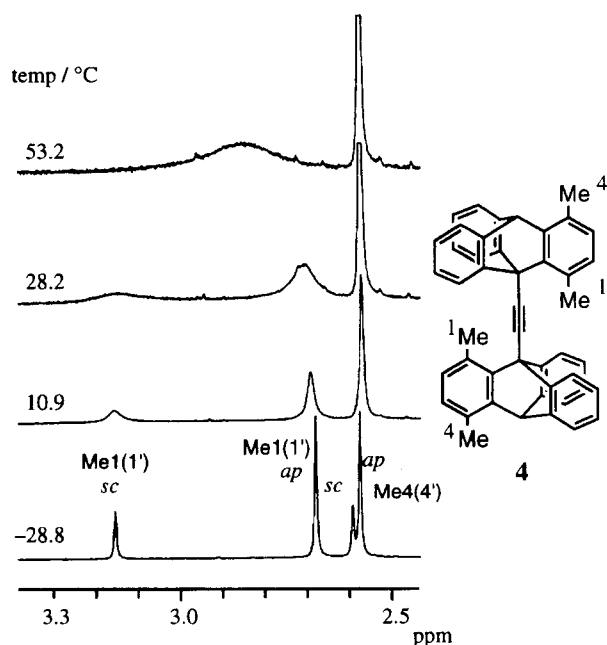


Fig. 2. ^1H NMR signals due to methyl protons in **4** at various temperatures (Solvent CDCl_3).

Table 2. Thermodynamic Parameters for Equilibrium between *ap* and *sc* Rotamers in **4**–**6** in CD_2Cl_2 ^{a)}

Compound	ΔH°	ΔS°	ΔG_{273}° ^{b)}	ΔG_{168}° ^{b)}	$\text{SE}(\text{sc}-\text{ap})$ ^{c)}
	kcal mol^{-1}	$\text{cal mol}^{-1} \cdot \text{K}^{-1}$	kcal mol^{-1}	kcal mol^{-1}	kcal mol^{-1}
4 ^{d)}	0.8 ± 0.2	-0.2 ± 0.6	0.88	0.86	1.87
			(1 : 0.40)	(1 : 0.15)	
5	-0.9 ± 0.2	-2.3 ± 0.8	-0.27	-0.52	0.93
			(1 : 3.3)	(1 : 9.5)	
6				-0.47	0.17
				(1 : 8.1)	

a) Data from *ap* to *sc* isomer. The statistical distributions of the two isomers were taken into account in the calculation. b) Values in parentheses are the rotamer populations (*ap* : *sc*) at the temperature. c) Relative steric energy of *sc* from *ap* isomer obtained by MM3 calculation. d) In CDCl_3 .

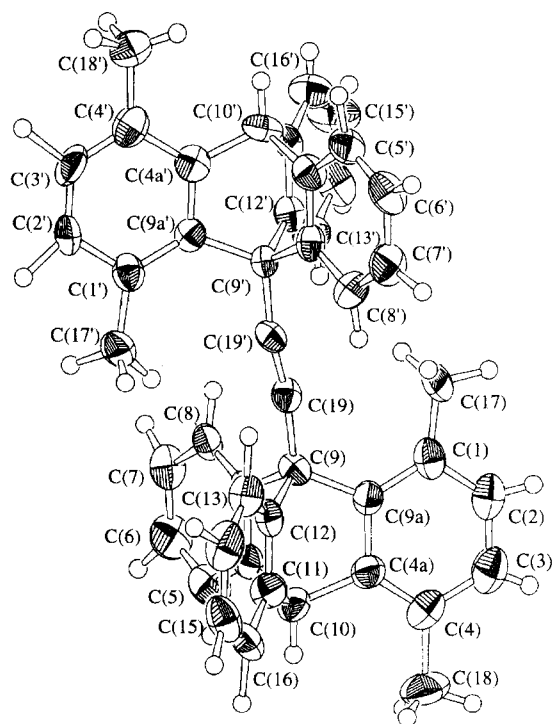


Fig. 3. ORTEP drawing of **4** with thermal ellipsoids at 50% probabilities (Solvent molecules are omitted for simplicity).

MM3* force-field parameters for the *ap* and *sc* forms of **4**, **5**, and **6**. The structural parameters of **4** are listed together with the experimental values in Table 3. The optimized structures of the *sc* forms of **4–6** are shown in Fig. 4. The relative steric energies between the two isomers are listed in Table 2.

Discussion

Molecular Structure. The X-ray structure of **4** shows that molecules take *ap* conformation in the solid state. The acetylenic carbons are significantly deformed from the linear arrangement: The bond angles at C(19) and C(19'), ca. 171°, are one of the most strained acetylenic carbons in non-conjugated acyclic alkynes.¹⁰ The torsion angle along the central axis indicates that the acetylenic moiety deforms into a zig-zag form. These deformations are attributable to the steric interaction between the two triptycyl groups. The distances of the triple bond and the attaching single bonds are in the normal ranges.

A notable difference between the X-ray and calculated structures of *ap*-**4** is the bond angles at the sp carbons: The calculated values are close to 180°. The underestimation of the bending deformation by the MM calculation can perhaps be attributed to the quality of the force-field parameters for highly strained acetylenic carbons. The calculation predicts that the bending deformation is significant for *sc*-**4**, of which the steric energy is larger by 1.9 kcal mol⁻¹ than that of the *ap* isomer, the value being also an overestimation to some extent.

¹³C NMR signals of the acetylenic carbons were observed at $\delta = 88$ –90 for **2** and **4**, this value being comparable to those in ethynes carrying *t*-alkyl substituents at both ends, for example 2,2,5,5-tetramethyl-3-hexyne at $\delta = 87$.¹³ At -36 °C, where the exchange was slow, **4** gave two acetylenic carbon signals assigned to the *ap* and *sc* isomers at $\delta = 89.4$ and 90.3, respectively, the latter being slightly but significantly deshielded than the former. If we can apply the general ten-

Table 3. Selected Structural Parameters of *ap* and *sc* Forms of **4** Determined by X-Ray Analysis and Molecular Mechanics (MM) Calculations

	<i>ap</i> - 4 (X-ray) ^{a)}	<i>ap</i> - 4 (MM) ^{b)}	<i>sc</i> - 4 (MM) ^{b)}
Bond distances (Å)			
C(19)–C(19')	1.19(1)	1.215	1.217
C(9)–C(19)	1.46(1)	1.479	1.484
C(9)–C(8a)	1.57(1)	1.528	1.530
C(9)–C(9a)	1.55(1)	1.530	1.531
C(9)–C(12)	1.54(1)	1.528	1.529
C(9a)–C(1)	1.40(1)	1.406	1.405
C(1)–C(17)	1.50(2)	1.508	1.506
Bond angles (°)			
C(9')–C(19')–C(19)	170.2(10)	177.0	170.5
C(19')–C(19)–C(9)	171.4(10)	177.0	170.5
C(19)–C(9)–C(9a)	119.6(8)	119.0	120.5
C(19)–C(9)–C(8a)	110.3(7)	109.7	108.7
C(19)–C(9)–C(12)	111.2(5)	109.7	109.7
C(9a)–C(9)–C(8a)	105.8(5)	105.6	105.5
C(9a)–C(9)–C(12)	104.7(7)	105.6	106.3
C(8a)–C(9)–C(12)	103.9(7)	106.6	105.5
C(9a)–C(1)–C(17)	126.3(9)	123.4	123.1
Torsion angles (°)			
C(9)–C(19)–C(19')–C(9')	–179(3)	–175.3	–14.5

a) Values in parentheses are estimated standard deviations. b) Optimized structures by MM3 calculation.

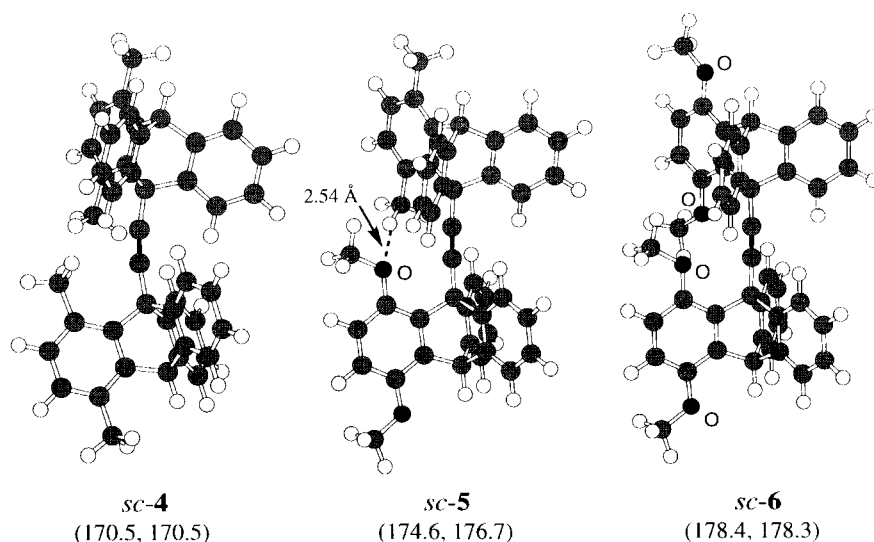


Fig. 4. Optimized structures of *sc* forms of **4**—**6** by MM3 calculations (Values in parentheses are bond angles at the top and bottom *sp* carbons, respectively, in $^{\circ}$).

dency that the bending deformation causes the chemical shift of the acetylenic signals toward downfield,^{14,15} this finding means that the deformation should be more severe in the *sc* isomer.

Rotational Barrier. The rotational barrier in **4** reported earlier ($15.6 \text{ kcal mol}^{-1}$)⁷ was excellently reproduced by our measurement with an NMR instrument at a high-magnetic field. Thanks to the good separation of the signals of each isomer, we could determine the rate constants over a wide temperature range to give the enthalpy and entropy of activation with reasonable reliability. Because the entropy of activation is not far from zero in each case, as expected for internal rotation, the enthalpy of activation plays a dominant role in determining the barrier height.

Table 1 clearly indicates that the rotational barrier is enhanced as the steric size of the substituent becomes large. For example, when the kinetic data of the compounds of *Y* (or *X*) = Me are compared, the free energy of activation increases in the order of **2**, **5**, and **4**, in which the substituents on the other Trip are H (1.20), OMe (1.52), and Me (1.80), respectively, the effective van der Waals radius (\AA) being indicated in parentheses.¹⁶ This tendency means that the transition state of the bond rotation is destabilized more than the initial state by the steric interaction. As expected from the general conformational analysis of ethane-type molecules, the two Trip moieties will be completely or nearly eclipsed at the transition state for rotation in bis(9-triptycyl)ethynes. In such structures, the steric interactions between the *peri* substituents on the two triptycyl groups reach a maximum even though the acetylene moiety can deform further so as to release the severe steric congestion.¹⁷

As shown in Scheme 2(a), when the C—C bond rotates from one staggered form to another in any direction by 120° , the *peri* substituents in the substituted Trip, *Y* and two H's, should pass over any *peri* hydrogens in the other Trip for **2** and **3**. Because the steric interaction of *Y* is most important among the nonbonding interactions at the transition state, its

steric size mainly influences the rotational barrier. For compounds **4**—**6** ($X \neq \text{H}$ and $Y \neq \text{H}$), both the substituents *X* and *Y* interact with the *peri* hydrogens during the rotation from *ap* to *sc*, whereas *X* should interact with *Y* during the isomerization between the two *sc* forms. From a steric viewpoint, the latter process requires much larger activation energy than the former. Namely, the relationship k_1 (or k_{-1}) $\gg k_2$ holds in the process shown in Scheme 2(b), and the rate constants observed by the lineshape analysis should correspond to k_1 . Therefore, the steric bulk of both *X* and *Y* is important in determining the rotational barriers in these compounds. The above discussion implies that the introduction of larger and more substituents at the *peri* positions can make the rotational barriers higher. Further study along this line is in progress.

The comparison of these data with those of bis(9-triptycyl)methane¹⁸ or *cis*-1,2-bis(9-triptycyl)ethene¹⁹ derivatives is meaningful to evaluate the interaction between two 9-triptycyl groups. The activation energies for the isomerization caused by the slippage of two triptycyl groups are ca. 30 kcal mol^{-1} for the methane and ethene analogs, even though the molecules carry no *peri* substituents. Although the experimental value is not available for **1**, its barrier, at least smaller than that in **3**, is much smaller than those in the above two compounds. The finding is readily understood by the spatial arrangement of the two triptycyl groups. In the ethyne compound, they are oriented far by being attached to both ends of ethyne to diminish the interactions. The distances between the two 9-bridgehead carbons are 4.1 and 3.0 \AA for the ethyne (**4**) and ethene compounds, respectively.

Rotamer Population. The thermodynamic data in Table 2 indicate that the *ap* form is more stable than the *sc* for **4** as expected from the steric interaction between the 1-methyl groups. The trend is reproduced by the MM calculation, although the energy gap between the two isomers ($1.9 \text{ kcal mol}^{-1}$) is a little larger than the experimental one ($0.9 \text{ kcal mol}^{-1}$).

On the contrary, the stability of the two isomers is vice

versa for the methoxy- containing compounds, **5** and **6**. We have to consider other factors stabilizing the *sc* form in these compounds.

A possible explanation is the C–H···O interaction in the *sc* form, which has been recognized in various 9-alkyl-1-methoxytritycenes.²⁰ In the calculated structure of *sc*-**5**, one of the 1-Me hydrogens is close to the oxygen in the 1'-OMe with the interatomic distance of 2.54 Å, which is within the sum of van der Waals radii of H and O atoms. This might indicate the presence of the C–H···O interaction in the *sc* form, although it was reported that the MM3 calculation could not evaluate the weak interaction correctly.²¹ As for the tetramethoxy compound (**6**), there are no significant H···O contacts (> 3.4 Å) in the calculated structure of *sc*-**6**; the C–H···O interaction is unlikely.²² Another plausible reason is the attractive dipole–dipole interaction between the two C–O–C moieties in the *sc* form. However, we could not obtain supporting evidence, though the effect of solvent polarity on the rotamer population would lend a clue, owing to the solubility problem. Further study is awaited on this point.

Experimental

¹H and ¹³C NMR spectra were measured on a Varian Gemini-300 at 300 and 75 MHz, respectively. Some ¹³C NMR spectra were measured on a JEOL Lambda 500 instrument at 125 MHz. The variable temperature NMR spectra were measured on a JEOL GSX-400 at 400 MHz. Unless otherwise noted, the NMR data were collected at room temperature. Melting points are uncorrected. Elemental analyses were performed by a Perkin–Elmer 2400-type analyzer. High-resolution mass spectra were measured on a JEOL JMS-700 MStation spectrometer.

9-[(Trimethylsilyl)ethynyl]anthracene (8). To a solution of 0.94 mL (6.7 mmol) of (trimethylsilyl)acetylene in 11 mL of dry ether was added 3.8 mL (6.2 mmol) of butyllithium solution in hexane at 0 °C under a nitrogen atmosphere. After the solution was stirred for 30 min at room temperature, 584 mg (3.01 mmol) of 9-anthrone was added to the flask and the whole was heated overnight under reflux. The mixture was quenched with ca. 10 mL of aqueous ammonium chloride. The organic layer was separated, and the aqueous layer was extracted with benzene. The combined organic solution was washed with aqueous NaCl, dried over MgSO₄, and evaporated. The residue mainly consisted of 9-[(trimethylsilyl)ethynyl]-9-anthrol, which was dehydrated during the purification by chromatography on silica gel (hexane eluent) to form the desired anthracene. The yield was 0.73 g (85%). The pure material was a pale yellow oil, which crystallized upon standing. The analytical sample was obtained by sublimation. Mp 61.0–62.0 °C. Found: C, 82.97; H, 6.69%. Calcd for C₁₉H₁₈Si: C, 83.16; H, 6.61%. ¹H NMR (CDCl₃) δ = 0.49 (9H, s), 7.50 (2H, t, *J* = 7.5 Hz), 7.59 (2H, dt, *J* = 0.8, 7.5 Hz), 8.00 (2H, dd, *J* = 0.8, 8.3 Hz), 8.42 (1H, s), 8.56 (2H, d, *J* = 8.3 Hz). ¹³C NMR (CDCl₃) δ = 0.28, 101.57, 106.16, 117.08, 125.60, 126.66, 126.74, 127.86, 128.61, 131.03, 132.87.

9-[(Trimethylsilyl)ethynyl]tritycene (10a). A solution of 1.10 g (4.00 mmol) of 9-[(trimethylsilyl)ethynyl]anthracene (**8**) in 10 mL of 1,2-dimethoxyethane (DME) was refluxed in a flask. To the solution were added a solution of 2.74 g (20.0 mmol) of anthranilic acid in 10 mL of DME and a solution of 3.51 g (30.0 mmol) of isopentyl nitrite in 10 mL of DME from respective dropping

funnels in 1.5 h. The mixture was further refluxed for 2 h. The volatile materials were removed by evaporation and the residue was chromatographed on silica gel (eluent hexane–dichloromethane). The elution of the starting anthracene was followed by that of the desired material. Recrystallization from hexane–dichloromethane gave 591 mg (42%) of the pure material as colorless crystals, and 260 mg of **8** was recovered. Mp 179–181 °C. Found: C, 85.35; H, 6.57%. Calcd for C₂₅H₂₂Si: C, 85.66; H, 6.33%. ¹H NMR (CDCl₃) δ = 0.46 (9H, s), 5.39 (1H, s), 6.98–7.09 (6H, m), 7.36 (3H, dd, *J* = 6.4, 2.1 Hz), 7.70 (3H, dd, *J* = 6.6, 1.9 Hz). ¹³C NMR (CDCl₃) δ = 0.38, 53.23, 53.76, 97.62, 100.05, 122.44, 123.32, 125.15, 125.62, 144.13, 144.38.

1,4-Dimethyl-9-[(trimethylsilyl)ethynyl]tritycene (10b). This compound was similarly prepared as above from the anthracene **8** and 3,6-dimethylantranilic acid²³ in 55% yield. The pure material was colorless powder. Mp 168–170 °C. Found: C, 85.99; H, 6.84%. Calcd for C₂₇H₂₆Si: C, 85.66; H, 6.92%. ¹H NMR (CDCl₃) δ = 0.42 (9H, s), 2.47 (3H, s), 2.81 (3H, s), 5.61 (1H, s), 6.56 and 6.64 (2H, ABq, *J* = 7.8 Hz), 7.06 (2H, dt, *J* = 1.6, 7.3 Hz), 7.09 (2H, dt, *J* = 1.3, 7.5 Hz), 7.36 (2H, dd, *J* = 7.1, 1.5 Hz), 7.83 (2H, dd, *J* = 7.3, 1.3 Hz). ¹³C NMR (CDCl₃) δ = –0.12, 18.84, 21.33, 49.76, 53.40, 98.38, 103.64, 123.02, 123.11, 125.09, 125.57, 126.85, 128.87, 129.43, 131.87, 140.60, 143.50, 144.15, 144.97.

1,4-Dimethoxy-9-[(trimethylsilyl)ethynyl]tritycene (10c). This compound was similarly prepared as **10a** from the anthracene **8** and 3,6-dimethoxyanthranilic acid²⁴ in 19% yield. The compound was purified by recrystallization from hexane–dichloromethane to give colorless crystals. Mp 215–217 °C. Found: C, 78.97; H, 6.57%. Calcd for C₂₇H₂₆O₂Si: C, 78.98; H, 6.38%. ¹H NMR (CDCl₃) δ = 0.44 (9H, s), 3.76 (3H, s), 3.81 (3H, s), 5.87 (1H, s), 6.54 and 6.55 (2H, ABq, *J* = 8.9 Hz), 7.02 (2H, dt, *J* = 1.0, 7.1 Hz), 7.07 (2H, dt, *J* = 1.4, 7.5 Hz), 7.38 (2H, dd, *J* = 1.7, 6.8 Hz), 7.84 (2H, dd, *J* = 1.7, 7.0 Hz). ¹³C NMR (CDCl₃) δ = 0.41, 46.21, 51.01, 56.23, 58.32, 95.36, 102.05, 109.70, 112.95, 123.03, 123.35, 125.01, 125.50, 133.83, 135.21, 144.39, 145.07, 149.01, 150.35.

9-Ethynyltritycene (11a). To a solution of 591 mg (1.69 mmol) of 9-[(trimethylsilyl)ethynyl]tritycene in 5 mL of THF was added 0.17 mL (1.7 mmol) of 1.0 mol L^{–1} solution of tetrabutylammonium fluoride in THF. The solution was stirred for 30 min at room temperature. The solvent was removed by evaporation, and the residue was treated with 10 mL of dichloromethane and 10 mL of water containing a few drops of acetic acid. The organic layer was separated, dried over MgSO₄, and evaporated. Recrystallization from hexane–dichloromethane afforded 432 mg (92%) of the pure material as colorless crystals. Mp 239–240 °C. Found: C, 94.70; H, 5.07%. Calcd for C₂₂H₁₄: C, 94.93; H, 5.07%. ¹H NMR (CDCl₃) δ = 3.27 (1H, s), 5.41 (1H, s), 6.99–7.09 (6H, m), 7.38 (3H, m), 7.74 (3H, m). ¹³C NMR (CDCl₃) δ = 52.92, 53.23, 78.43, 80.47, 122.33, 123.39, 125.19, 125.72, 143.86, 144.30.

11b and **11c** were similarly prepared from **10b** and **10c**, respectively.

9-Ethynyl-1,4-dimethyltritycene (11b). Yield 93%. Mp 196–199 °C. Found: C, 94.32; H, 6.06%. Calcd for C₂₄H₁₈: C, 94.08; H, 5.92%. ¹H NMR (CDCl₃) δ = 2.48 (3H, s), 2.81 (3H, s), 3.26 (1H, s), 5.63 (1H, s), 6.64 and 6.72 (2H, ABq, *J* = 7.7 Hz), 7.04 (2H, dt, *J* = 1.2, 7.6 Hz), 7.10 (2H, dt, *J* = 1.2, 7.6 Hz), 7.37 (2H, dd, *J* = 1.4, 6.9 Hz), 7.87 (2H, dd, *J* = 1.4, 7.6 Hz). ¹³C NMR (CDCl₃) δ = 18.85, 21.30, 49.75, 52.53, 81.57, 81.80, 122.93, 123.18, 125.11, 125.65, 126.93, 128.88, 129.61, 131.85, 140.31, 143.44, 144.05, 144.71.

9-Ethynyl-1,4-dimethoxytritycene (11c). Yield 94%. Mp

264–266 °C. Found: C, 84.91; H, 5.36%. Calcd for $C_{24}H_{18}O_2$: C, 85.18; H, 5.36%. 1H NMR ($CDCl_3$) δ = 3.21 (1H, s), 3.78 (3H, s), 3.81 (3H, s), 5.89 (1H, s), 6.56 and 6.58 (2H, ABq, J = 8.9 Hz), 7.03 (2H, dt, J = 1.5, 7.5 Hz), 7.08 (2H, dt, J = 1.5, 7.5 Hz), 7.40 (2H, dd, J = 6.7, 1.8 Hz), 7.88 (2H, dd, J = 6.9, 1.9 Hz). ^{13}C NMR ($CDCl_3$) δ = 46.22, 50.18, 56.30, 58.51, 78.74, 80.08, 109.87, 113.14, 122.91, 123.46, 125.06, 125.62, 133.58, 135.20, 144.30, 144.79, 149.12, 150.33.

9-[(9-Anthryl)ethynyl]triptycene (12a). In 10 mL of degassed triethylamine, 96 mg (0.35 mmol) of 9-ethynyltriptycene, 147 mg (0.48 mmol) of 9-iodoanthracene,²⁵ 17 mg (0.024 mmol) of $[PdCl_2(PPh_3)_2]$, and 2.5 mg (0.013 mmol) of CuI were suspended. The mixture was refluxed for 20 h under a nitrogen atmosphere. The solvent was removed by evaporation and the residue was submitted to chromatography on silica gel with hexane–dichloromethane 10:1–2:1 eluent. The fractions showing a bright fluorescence on TLC were collected, and this material was recrystallized from chloroform to give the desired compound as yellow powders in 78% yield. Mp 289–291 °C. Found: C, 94.78; H, 4.82%. Calcd for $C_{36}H_{22}$: C, 95.12; H, 4.88%. 1H NMR ($CDCl_3$) δ = 5.53 (1H, s), 7.10 (3H, dt, J = 1.6, 7.4 Hz), 7.13 (3H, dt, J = 1.6, 7.6 Hz), 7.47 (3H, m), 7.58 (2H, dt, J = 1.4, 6.8 Hz), 7.68 (2H, ddd, J = 1.4, 6.8, 7.6 Hz), 8.06 (3H, m), 8.13 (2H, d, J = 8.4 Hz), 8.58 (1H, s), 8.96 (2H, d, J = 8.4 Hz). ^{13}C NMR ($CDCl_3$) δ = 53.41, 54.64, 89.28, 95.24, 116.93, 122.71, 123.57, 125.39, 125.76, 125.83, 126.70, 127.11, 128.13, 128.90, 131.25, 133.12, 144.54, 144.71.

12b and **12c** were similarly prepared from **11b** and **11c**, respectively.

9-[(9-Anthryl)ethynyl]-1,4-dimethyltriptycene (12b). Yield 72%. Yellow crystals. Mp 294–295 °C. Found: C, 94.87; H, 5.55%. Calcd for $C_{38}H_{26}$: C, 94.57; H, 5.43%. 1H NMR ($CDCl_3$) δ = 2.54 (3H, s), 2.95 (3H, s), 5.74 (1H, s), 6.70 and 6.78 (2H, ABq, J = 8.0 Hz), 7.10 (2H, dt, J = 1.4, 7.5 Hz), 7.15 (2H, dt, J = 1.4, 7.5 Hz), 7.46 (2H, dd, J = 1.7, 6.7 Hz), 7.57 (2H, ddd, J = 1.1, 6.6, 7.9 Hz), 7.64 (2H, ddd, J = 1.4, 6.6, 7.9 Hz), 8.11 (2H, dd, J = 1.4, 7.7 Hz), 7.21 (2H, dd, J = 1.7, 7.1 Hz), 8.55 (1H, s), 8.92 (2H, dd, J = 1.1, 7.7 Hz). ^{13}C NMR ($CDCl_3$) δ = 18.91, 21.94, 50.02, 54.31, 90.53, 98.75, 117.41, 123.30, 123.42, 125.33, 125.73, 125.77, 126.73, 126.95, 127.07, 127.96, 128.92, 128.95, 129.65, 131.35, 131.74, 133.23, 141.10, 143.64, 144.39, 145.62.

9-[(9-Anthryl)ethynyl]-1,4-dimethoxytriptycene (12c). Yield 72%. Recrystallization from dichloromethane gave yellow crystals containing solvent molecules. Mp 350–353 °C. Found: C, 87.36; H, 5.02%. Calcd for $C_{38}H_{26}O_2 \cdot 1/8(CH_2Cl_2)$: C, 87.18; H, 5.04%. 1H NMR ($CDCl_3$) δ = 3.81 (3H, s), 3.86 (3H, s), 5.30 (1H, s), 6.63 and 6.66 (2H, ABq, J = 8.9 Hz), 7.04–7.13 (4H, m), 7.49 (2H, m), 7.52–7.64 (4H, m), 8.10 (2H, d, J = 7.5 Hz), 8.15 (2H, m), 8.53 (1H, s), 9.03 (2H, d, J = 8.9 Hz).

(1,4-Dimethyl-9-triptycyl)(9-triptycyl)ethyne (2). To a refluxing solution of 100 mg (0.207 mmol) of **12b** in 10 mL of DME were added a solution of 142 mg (1.03 mmol) of anthranilic acid in 5 mL of DME and a solution of 182 mg (1.55 mmol) of isopentyl nitrite in 5 mL of DME from respective dropping funnels in 1 h. The mixture was refluxed for 2 h. The volatile materials were removed by evaporation. The residue was submitted to a plug column on silica gel with hexane–dichloromethane eluent to give 105 mg of a mixture of the starting material and the Diels–Alder adducts. This mixture was further separated by another chromatography on silica gel with the same eluent system to afford 57 mg (49%) of the desired compound as colorless powder with 30 mg of recovery of **12b**. The corrected yield was 70%. The analytical sample was obtained by recrystallization from hexane–dichloromethane. Mp

420–438 °C (decomp). Found: C, 94.59; H, 5.41%. Calcd for $C_{44}H_{30}$: C, 94.69; H, 5.58%. 1H NMR ($CDCl_3$) δ = 2.56 (3H, s), 3.00 (3H, s), 5.54 (1H, s), 5.77 (1H, s), 6.71 and 6.80 (2H, ABq, J = 7.7 Hz), 7.04–7.14 (10H, m), 7.44–7.51 (5H, m), 8.01 (3H, m), 8.13 (2H, m). ^{13}C NMR ($CDCl_3$) δ = 18.96, 22.22, 49.94, 53.34, 53.43, 53.83, 87.83, 90.34, 122.58, 123.07, 123.43, 123.69, 125.49, 125.68, 125.81, 125.85, 127.16, 129.03, 129.74, 131.73, 140.50, 143.62, 144.34, 144.51, 145.49.

Bis(9-triptycyl)ethyne (1) was prepared from **12a** and anthranilic acid in 38% yield with the recovery of 22% of **12a**. Mp 425–435 °C (decomp) (lit, 450 °C).⁷ 1H NMR ($CDCl_3$) δ = 5.57 (2H, s), 7.09–7.12 (12H, m), 7.50 (6H, m), 8.04 (4H, m). HRMS (FAB) MH^+ Found: m/z 531.2122. Calcd for $C_{42}H_{26}$: MH^+ , 531.2113.

(1,4-Dimethoxy-9-triptycyl)(9-triptycyl)ethyne (3) was prepared from **12a** and 3,6-dimethoxyanthranilic acid in 36% yield with recovery of 40% of **12a**. Mp 395–415 °C (decomp). Found: C, 89.66; H, 5.22%. Calcd for $C_{44}H_{30}O_2$: C, 89.46; H, 5.12%. 1H NMR ($CDCl_3$) δ = 3.56 (3H, s), 3.87 (3H, s), 5.54 (1H, s), 6.02 (1H, s), 6.59 and 6.63 (2H, ABq, J = 8.9 Hz), 7.04–7.12 (10H, m), 7.44–7.52 (5H, m), 8.11 (3H, m), 8.16 (2H, m).

Bis(1,4-dimethyl-9-triptycyl)ethyne (4) was prepared from **12b** and 3,6-dimethylanthranilic acid in 37% yield with the recovery of 45% of **12b**. Mp 395–415 °C (decomp), (lit, 423 °C (decomp)).⁷ HRMS (FAB) MH^+ Found: m/z 587.2761. Calcd for $C_{46}H_{34}$: MH^+ 587.2739. 1H NMR ($CDCl_3$) δ = 2.56, 2.69 and 3.18 (12H, br), 5.77 (2H, s), 6.58–6.82 (4H, m), 7.14 (8H, br s), 7.50 (4H, br s), 8.30 (4H, br s). 1H NMR ($CDCl_3$, –55 °C) δ = 2.55 (6H_{ap}, s), 2.57 (6H_{sc}, s), 2.65 (6H_{ap}, s), 3.15 (6H_{sc}, s), 5.80 (2H, s), 6.63 (2H_{ap}, d, J = 7.9 Hz), 6.78 (2H_{ap}, d, J = 7.9 Hz), 6.75–6.91 (6H_{sc}, m), 7.04 (2H_{sc}, t, J = 6.8 Hz), 7.10–7.20 (8H_{ap} and 8H_{sc}, m), 7.48 (4H_{sc}, d, J = 7.5 Hz), 7.54 (4H_{ap}, m), 7.73 (4H_{sc}, d, J = 7.5 Hz), 8.27 (4H_{ap}, m). The rotamer population (*ap*:*sc*) was 3.29:1 at –55 °C. ^{13}C NMR ($CDCl_3$, 125 MHz) δ = 18.95, 22.0 (br), 49.94, 53.62, 89.95 (br), 123.22, 123.62, 125.35, 125.82, 127.10, 128.99, 129.62, 131.68, 141.0 (br), 143.64, 144.36, 144.6 (br). At –36 °C, the acetylenic carbon signals were observed at δ = 89.40 and 90.30 (ca. 3:1 intensity) assignable to *ap* and *sc* forms, respectively.

(1,4-Dimethoxy-9-triptycyl)(1,4-dimethyl-9-triptycyl)ethyne (5) was prepared from **12b** and 3,6-dimethoxyanthranilic acid in 72% yield with the recovery of 10% of **12b**. Mp 380–405 °C (decomp). Found: C, 89.29; H, 5.54%. Calcd for $C_{46}H_{34}O_2$: C, 88.98; H, 5.62%. 1H NMR ($CDCl_3$) δ = 2.55 (3H, s), 3.02 (3H, br), 3.54 (3H, br), 3.85 (3H, s), 5.75 (1H, s), 6.00 (1H, s), 6.55 and 6.62 (2H, ABq, J = 9.0 Hz), 6.71 and 6.78 (2H, ABq, J = 7.9 Hz), 6.99–7.12 (8H, m), 7.42–7.51 (4H, m), 8.19 (4H, m). 1H NMR (CD_2Cl_2 , –84 °C) δ = 2.47 (3H, s, Me_{sc}), 2.48 (3H, s, Me_{ap}), 2.64 (3H, s, Me_{ap}), 2.97 (3H, s, Me_{sc}), 3.01 (3H, s, OMe_{ap}), 3.58 (3H, s, OMe_{sc}), 3.73 (3H, s, OMe_{ap}), 3.78 (3H, s, OMe_{sc}), 6.42–8.32 (aromatic signals). The major isomer gave four sets of aromatic ABCD signals, being consistent with the stereochemistry of *sc*. The rotamer population (*ap*:*sc*) was 1:7.0 at the temperature.

Bis(1,4-dimethoxy-9-triptycyl)ethyne (6) was prepared from **12c** and 3,6-dimethoxyanthranilic acid in 19% yield with the recovery of 52% of **12c**. Recrystallization from dichloromethane afforded crystals containing solvent molecules. Mp 405–435 °C (decomp). Found: C, 80.32; H, 5.13%. Calcd for $C_{46}H_{34}O_4 \cdot 1/2(CH_2Cl_2)$: C, 80.57; H, 5.09%. 1H NMR ($CDCl_3$) δ = 3.55 (6H, s), 3.86 (6H, s), 6.00 (2H, s), 6.59 and 6.62 (4H, ABq, J = 8.9 Hz), 7.06 (8H, m), 7.48 (4H, m), 8.27 (4H, m). 1H NMR (CD_2Cl_2 , –105 °C) δ = 3.61 (3H, s), 3.75 (3H, s), 5.95 (2H, s), 6.59 and 6.67 (4H, ABq, J = 8.9 Hz), 6.90 (2H, t, J = 6.8 Hz), 6.98–7.13 (6H, m), 7.39–7.50 (4H, m), 7.84 (2H, d, J = 7.5 Hz), 8.45 (2H, m) for the *sc* isomer. Most

Table 4. Rate Constants of C–C Bond Rotation Determined by Total Lineshape Analysis^{a)}

Compound	k/s^{-1} (temp/°C)
2	12.0 (–89.6), 25 (–84.1), 52 (–79.1), 90 (–73.9), 160 (–68.8), 260 (–63.5), 450 (–58.3), 750 (–53.1), 1300 (–47.9)
4	4.3 (5.1), 7.5 (10.9), 13.0 (16.7), 22.5 (22.5), 37.5 (28.2), 65 (34.0), 100 (39.8), 150 (45.5)
5	4.8 (–46.8), 9.0 (–41.1), 17.5 (–35.1), 30 (–29.6), 52.5 (–23.9), 90 (–18.2), 150 (–12.2), 250 (–6.4)
6	15 (–93.7), 35 (–87.4), 90 (–80.0), 350 (–70.5), 1400 (–57.8), 5000 (–45.2)

a) The solvent was CDCl₃ for **4** and CD₂Cl₂ for the other compounds. For **4–6**, k 's are those from *ap* to *sc* isomers, namely k_1 in Scheme 2.

of the signals due to the *ap* isomer could not be read independently due to the overlapping, except for the signals at 3.17 (3H, s) and 8.20 (4H, m). The rotamer population (*ap*:*sc*) was 1:8.1 at the temperature.

Dynamic NMR Measurement. The samples were prepared by the dissolution of ca. 5 mg of a compound in 0.6 ml of a deuterated solvent for **2–4**. Because of the poor solubility, saturated solutions were used for the measurements of **5** and **6** (ca. 1 mg per sample). During the variable temperature measurements, the temperatures of the sample were read from a thermocouple after the calibration with chemical shift differences of the methanol signals. The total lineshape analysis was performed by the DNMR3K program.²⁶ The lineshapes were analyzed as an exchange of three sites of AX systems for **2** and **3**, and as that between unequally populated two sites for **4–6**. Chemical shift differences, coupling constants, and rotamer populations were measured at several temperatures, where the exchange was negligibly slow. The chemical shift differences were assumed to be correlated with the temperature linearly. The coupling constants were independent of the temperature in **2**. The rotamer population was analyzed by the van't Hoff equation for **4** and **5**. Spin–spin relaxation times (T_2 's) were estimated from the lineshapes at the slow exchange limit. The signal due to the *peri* protons in the nonsubstituted Trip in **3** was in the process of decoalescence at the lowest attainable temperature, –110 °C, in CD₂Cl₂, where the rate constant was estimated to be 100 s^{–1}, corresponding to 8.0 kcal mol^{–1} in the free energy of activation. For **6**, the dynamic process was practically frozen at –105 °C in CD₂Cl₂, and the chemical shift difference at the temperature was used for the lineshape analysis. The correlation of the chemical shift difference ($\Delta\nu$) with the temperature ($t/^\circ\text{C}$), the coupling constants (J), and the T_2 values for each compound are as follows. **2**: $\Delta\nu = 175.0\text{ Hz}$, $J = 6.8\text{ Hz}$, $T_2 = 0.10\text{--}0.12\text{ s}$. **4**: $\Delta\nu = -0.099t + 197.3\text{ Hz}$, $T_2 = 0.14\text{ s}$. **5**: $\Delta\nu = -0.086t + 118.66\text{ Hz}$, $T_2 = 0.12\text{--}0.14\text{ s}$. **6**: $\Delta\nu = 179.0\text{ Hz}$, $T_2 = 0.08\text{--}0.10\text{ s}$. The rate constants are listed in Table 4.

X-Ray Analysis of **4.**²⁸ A crystal used for the X-ray measurement was grown from a chloroform solution, and contains two solvent molecules with respect to one molecule of **4**. The crystal size was 0.15×0.10×0.10 mm³. X-Ray measurement was performed on a Rigaku AFC7R four circle diffractometer with Cu K α radiation ($\lambda = 1.54178\text{ \AA}$) at room temperature. The scan mode was the ω –2 θ method and the scan rate was 10.0° min^{–1} in ω . The scan range was calculated by $0.79^\circ + 0.30^\circ \tan \theta$. The structure was solved by the direct method and refined by the full-matrix least-squares method by using a TEXSAN program.

Anisotropic thermal parameters were employed for non-hydrogen atoms and isotropic ones for hydrogens. The reflection data were corrected for the Lorentz-polarization effects and secondary extinction. The total number of measured unique reflections was 3408 in the range of $2^\circ < 2\theta < 120^\circ$ and 3270 reflections were used for the structure determination and refinement. The function minimized was $\sum[w(|F_o| - |F_c|)^2]$, where $w = [\sigma_c^2|F_o| + (p^2/4)|F_o|^2]^{-1}$ and p -factor = 0.096. The parameters of some atoms were fixed during the refinement. The carbon and chlorine atoms in solvent molecules occupied multiple positions due to disorder. Formula C₄₈H₃₆Cl₆, F.W. 825.53, Monoclinic, Space group $P2_1$ (#4), $a = 15.592(2)$, $b = 8.642(2)$, $c = 16.677(2)\text{ \AA}$, $\beta = 114.773(9)^\circ$, $V = 2040.4(6)\text{ \AA}^3$, $Z = 2$, $D_c = 1.344\text{ g cm}^{-3}$, $\mu(\text{Cu K}\alpha) = 40.95\text{ cm}^{-1}$, R 0.089, R_w 0.068.

MM Calculation. The calculations were carried out by Macro-Model ver. 6.0 program²⁹ with a Silicon Graphics INDIGO2 workstation. The MM3* force-field parameters were used without modification. The optimized structures were initiated by Chem3D program on a Macintosh computer.

The present work was partly supported by a fund from Japan Private School Promotion Foundation and by a Grant-in-Aid for Scientific Research on Priority Areas (A) "Creation of Delocalized Electronic Systems" No. 10146254 from the Ministry of Education, Science, Sports and Culture.

References

- 1 E. L. Eliel, S. H. Wilen, and L. N. Mander, "Stereochemistry of Organic Compounds," Wiley, New York (1994), Chap. 10.
- 2 M. Ōki, "The Chemistry of Rotational Isomers," Springer-Verlag, New York (1993), Chap. 3.
- 3 M. Ōki, "Applications of Dynamic NMR Spectroscopy to Organic Chemistry," VCH, Deerfield Beach (1985), Chap. 6.
- 4 S. Sternhell, in "Dynamic Nuclear Magnetic Resonance Spectroscopy," ed by L. M. Jackman and F. A. Cotton, Academic Press, New York (1975), Chap. 6.
- 5 B. T. Luke, J. A. Pople, M.-B. Krogh-Jespersen, Y. Apeloig, J. Chandrasekhar, and P. v. R. Schleyer, *J. Am. Chem. Soc.*, **108**, 260 (1986); W. J. Hehre, L. Radom, P. v. R. Schleyer, and J. A. Pople, "Ab Initio Molecular Orbital Theory," John Wiley & Sons, New York (1986), Chap. 6.4.
- 6 W. B. Olson and D. Papousek, *J. Mol. Spectrosc.*, **37**, 527

(1971); K. Okuyama, T. Hasegawa, M. Ito, and N. Mikami, *J. Phys. Chem.*, **88**, 1711 (1984).

7 P. Koo Tze Mew and F. Vögtle, *Angew. Chem., Int. Ed. Engl.*, **18**, 159 (1979).

8 S. Takahashi, Y. Kuroyama, K. Sonogashira, and N. Hagihara, *Synthesis*, **1980**, 627.

9 The symbols of *ap* (antiperiplanar) and *sc* (synclinal) were originally proposed for the designation of the conformation about C–C single bonds according to the IUPAC recommendation: J. Rigaudy and S. P. Klesney, "Nomenclature of Organic Chemistry, 1979 Edition," Pergamon Press, Oxford (1979), Sect. E. We use these symbols for the conformation along an acetylenic moiety (C–C≡C–C) comprised of two single bonds and one triple bond as the authors of Ref. 7 did, because this usage makes no confusion as far as the central axis is not bent seriously.

10 The Cambridge Crystallographic Database analysis with the substructure of acyclic C(sp³)–C≡C–C(sp³) provided 20 hits, which show the bond angles smaller than 176°. The smallest four examples (171.6–172.0°) are propargyl alcohol derivatives with guest molecules. The next two are acetylenes with no functional groups at the α -positions: 7,8-bis(3,3-dimethyl-1-butyryl)-*cis-transoid-cis*-tricyclo[6.4.0.0^{2,7}]dodecan-3,12-dione (172.2 and 172.8°)¹¹ and 4-octadecynoic acid (172.6 and 173.0°).¹²

11 H.-J. Rathjen, W. C. Agosta, P. Margaretha, A.-M. Chiu, L. Todaro, and S. Wolff, *Acta Crystallogr., Sect. C*, **C47**, 2176 (1991).

12 F. Mo, *Acta Crystallogr., Sect. B*, **B35**, 2135 (1979).

13 J. -E. Dubois and J. -P. Doucet, *J. Chem. Res. (M)*, **1980**, 1101.

14 E. Breitmaier and W. Voelter, "Carbon-13 NMR Spectroscopy," 3rd ed, VCH, New York (1990), Chap. 4.3.

15 For recent examples of the low-field shift of the acetylenic carbon signals by the bending deformation, see: T. Kawase, N. Ueda, H. R. Darabi, and M. Oda, *Angew. Chem., Int. Ed. Engl.*, **35**, 1556 (1996); T. Kawase, H. R. Darabi, and M. Oda, *Angew. Chem., Int. Ed. Engl.*, **35**, 2664 (1996).

16 R. Cosmo and S. Sternhell, *Aust. J. Chem.*, **40**, 35 (1987); G. Bott, L. D. Field, and S. Sternhell, *J. Am. Chem. Soc.*, **102**, 5618 (1980).

17 In a rigid molecular model, the *peri* substituents interact severely in the eclipsed conformations.

18 H. Iwamura and K. Mislow, *Acc. Chem. Res.*, **21**, 175 (1988).

19 Y. Kawada, H. Sakai, M. Oguri, and G. Koga, *Tetrahedron*

Lett., **35**, 139 (1994).

20 Ref. 2, pp. 38–42 and references therein. M. Ōki, N. Takiguchi, S. Toyota, G. Yamamoto, and S. Murata, *Bull. Chem. Soc. Jpn.*, **61**, 4295 (1988); S. Toyota, M. Endo, M. Teruhi, Y. Noda, M. Ōki, M. Yamasaki, and T. Shibahara, *Bull. Chem. Soc. Jpn.*, **66**, 2088 (1993); S. Toyota, T. Miyasaka, Y. Matsumoto, T. Matsuo, and M. Ōki, *Bull. Chem. Soc. Jpn.*, **67**, 1680 (1994); S. Toyota, Y. Watanabe, H. Yoshida, and M. Ōki, *Bull. Chem. Soc. Jpn.*, **68**, 2751 (1995).

21 K. Sakakibara and N. L. Allinger, *J. Org. Chem.*, **60**, 4044 (1995).

22 A referee pointed out that the C–H···O interaction between the 1-methoxy oxygens and the *peri*-hydrogen atoms was another possible factor influencing the rotamer population in **6**. However, there are no important contacts between the O and H atoms (> 2.92 Å) in the optimized structures of the *ap* and *sc* forms by the MM calculation. In order to consult this kind of weak interactions, the structure should be optimized by the MO calculations including the electronic interactions. We failed to run the MO calculation of this molecule due to the limitation of the molecular size even though a simplified model compound was input. Further studies of this series will shed light on the point.

23 G. Gronowitz and G. Hansen, *Ark. Kemi.*, **27**, 145 (1967).

24 M. Ōki, Y. Tanaka, G. Yamamoto, and N. Nakamura, *Bull. Chem. Soc. Jpn.*, **56**, 302 (1983).

25 K. Matsui, E. Tobita, M. Ando, and K. Kondo, *Chem. Lett.*, **1981**, 1719.

26 A modified version of DNMR3 program²⁷ by Prof. H. Kihara of Hyogo University of Teacher Education for NEC personal computers.

27 G. Binsch, *Top. Stereochem.*, **3**, 97 (1968). D. Kleier and G. Binsch, "QCPE #165," Indiana University, Bloomington.

28 Tables of positional and thermal parameters and bond lengths and angles for nonhydrogen atoms have been deposited as Document No. 73011 at the Office of the Editor of the Bull. Chem. Soc. Jpn. Crystallographic data have been also deposited at the CCDC, 12 Union Road, Cambridge CB2 1EZ, UK and copies can be obtained on request, free of charge, by quoting the publication citation and the deposition number CCDC 136571.

29 F. Mohamadi, N. G. J. Richards, W. C. Guida, R. Liskamp, M. Lipton, C. Caufield, G. Chang, T. Hendrickson, and W. C. Still, *J. Comput. Chem.*, **11**, 440 (1990).